

Supporting Information

Selective Atomic Layer Deposition of RuO_x Catalysts on Shape-Controlled Pd Nanocrystals with Significantly Enhanced Hydrogen Evolution Activity

Lei Zhang^{1, a}, Zhi-Jian Zhao^{1, b}, Mohammad Norouzi Banis^{1, a}, Lulu Li,^b Yang Zhao,^a Zhongxin Song,^a Zhiqiang Wang,^c Tsun-Kong Sham,^c Ruying Li,^a Matthew Zheng,^a Jinlong Gong,^b and
Xueliang Sun^{*a}

a Department of Mechanical and Materials Engineering, The University of Western Ontario, London, ON N6A 5B9, Canada

b Key Laboratory for Green Chemical Technology of Ministry of Education, School of Chemical Engineering and Technology, Tianjin University; Collaborative Innovation Center of Chemical Science and Engineering (Tianjin), Tianjin 300072, P.R. China.

c Department of Chemistry, University of Western Ontario, London, ON, N6A 5B7, Canada

Corresponding Email: xsun@eng.uwo.ca

1 These authors contributed equally to this work.

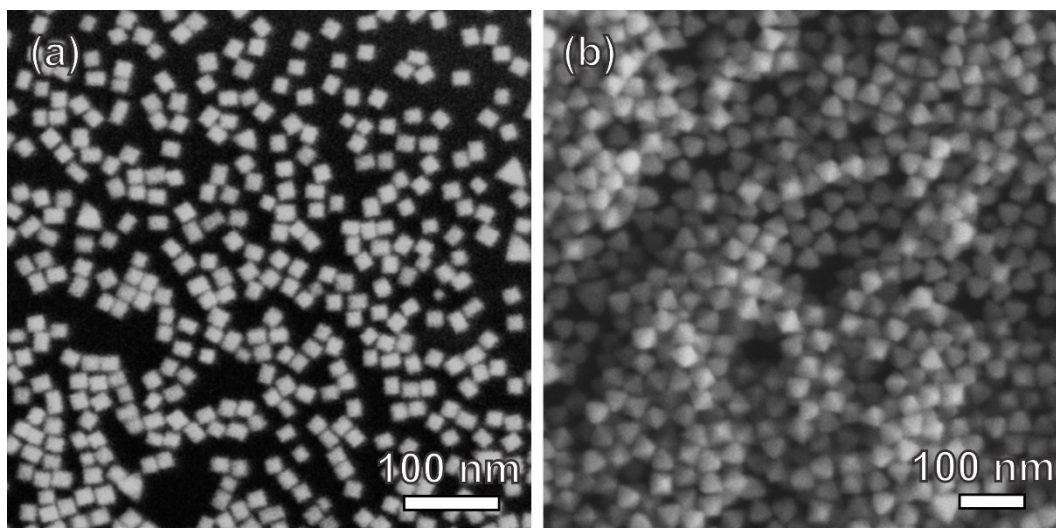


Fig. S1. SEM images of (a) Pd nanocubes and (b) octahedrons that were used as substrate for the ALD deposition of Ru atoms.

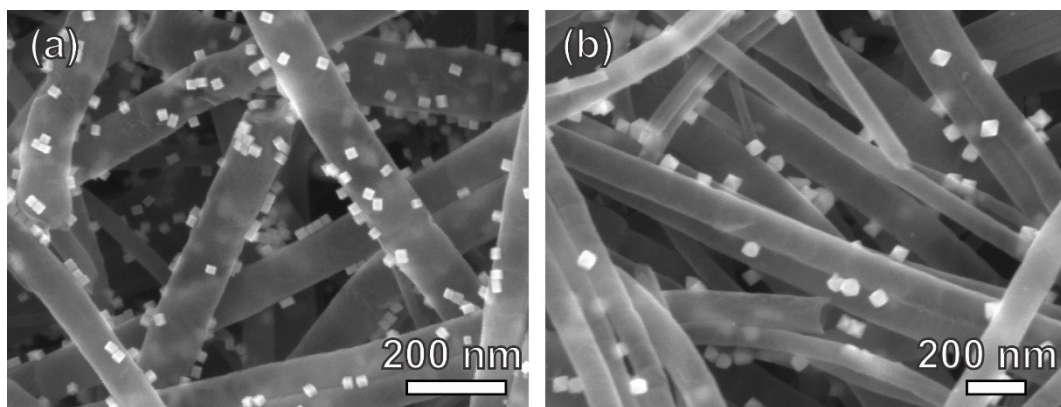


Fig. S2. SEM images of (a) Pd nanocubes and (b) octahedrons that were loaded on NCNT with a mass ratio of 20%.

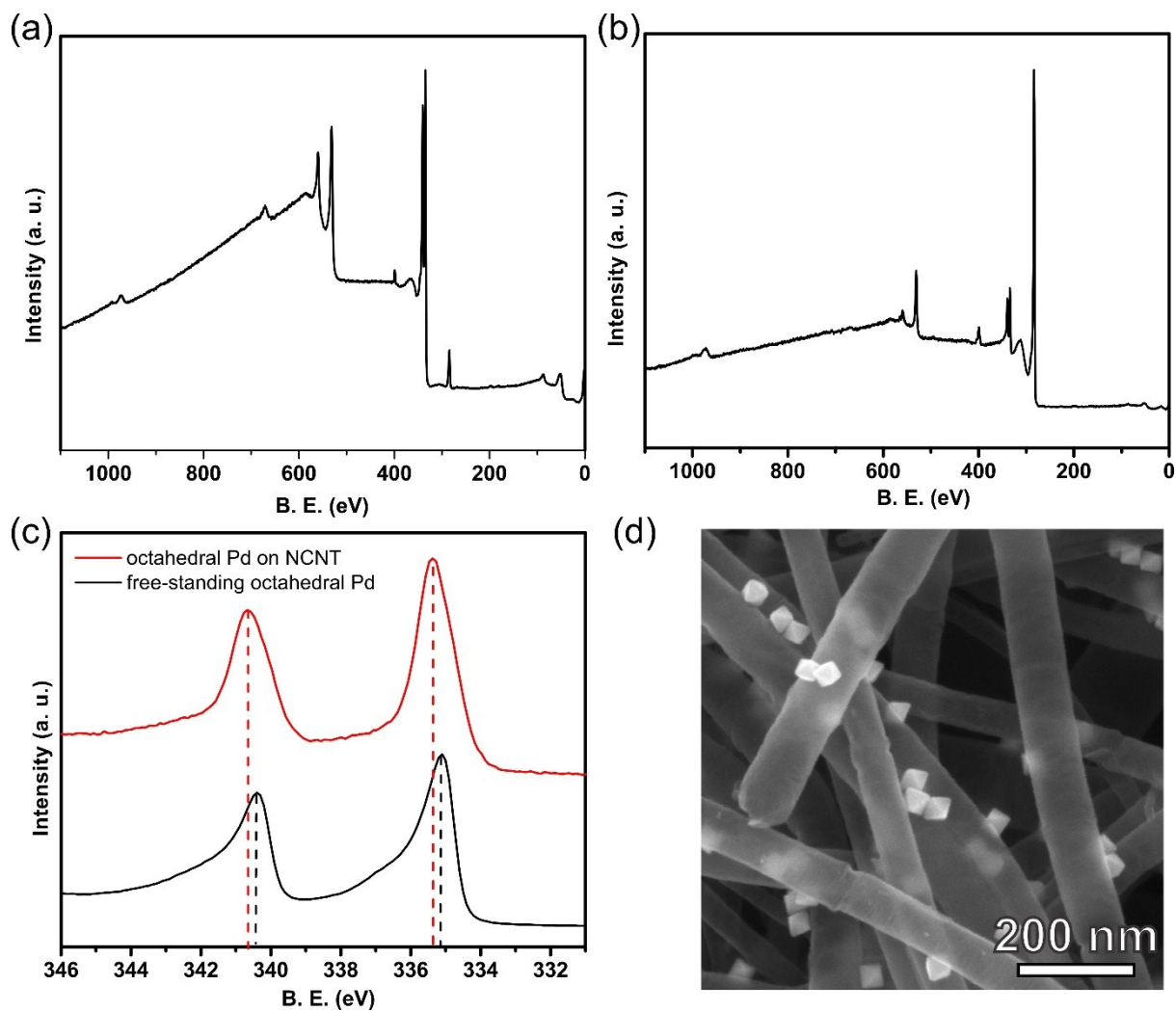


Fig. S3. XPS tests of (a) octahedral Pd on NCNT, (b) free standing Pd octahedrons and (c) Pd 3d spectra. (d) SEM image of octahedral Pd/NCNT after heating in ALD chamber for 1 h.

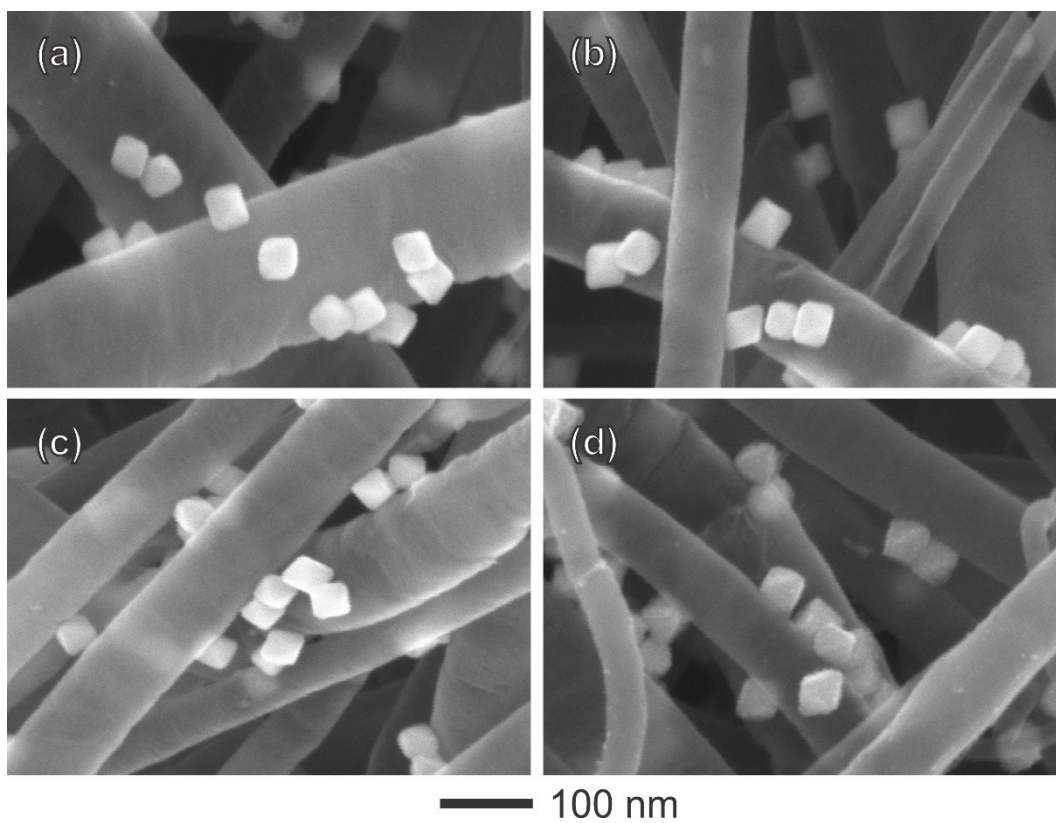


Fig. S4. SEM images of Pd@RuO_x nanocrystals on NCNT that were prepared by depositing Ru on Pd octahedrons/NCNT at various ALD cycles: (a) 10, (b) 20, (c) 30, and (d) 50 cycles, respectively.

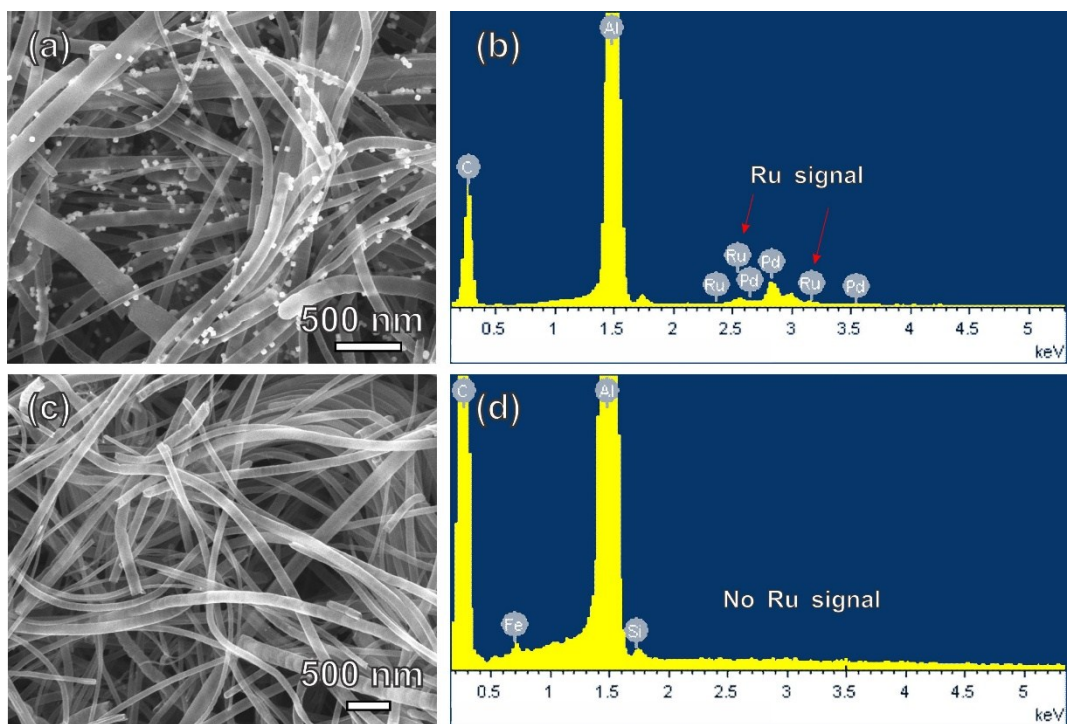


Fig. S5. The SEM and corresponding EDX spectra of (a, b) Pd/NCNT and (c, d) pure NCNT after ALD of Ru for 30 cycles, indicating Ru atoms were selectively deposited on Pd particles.

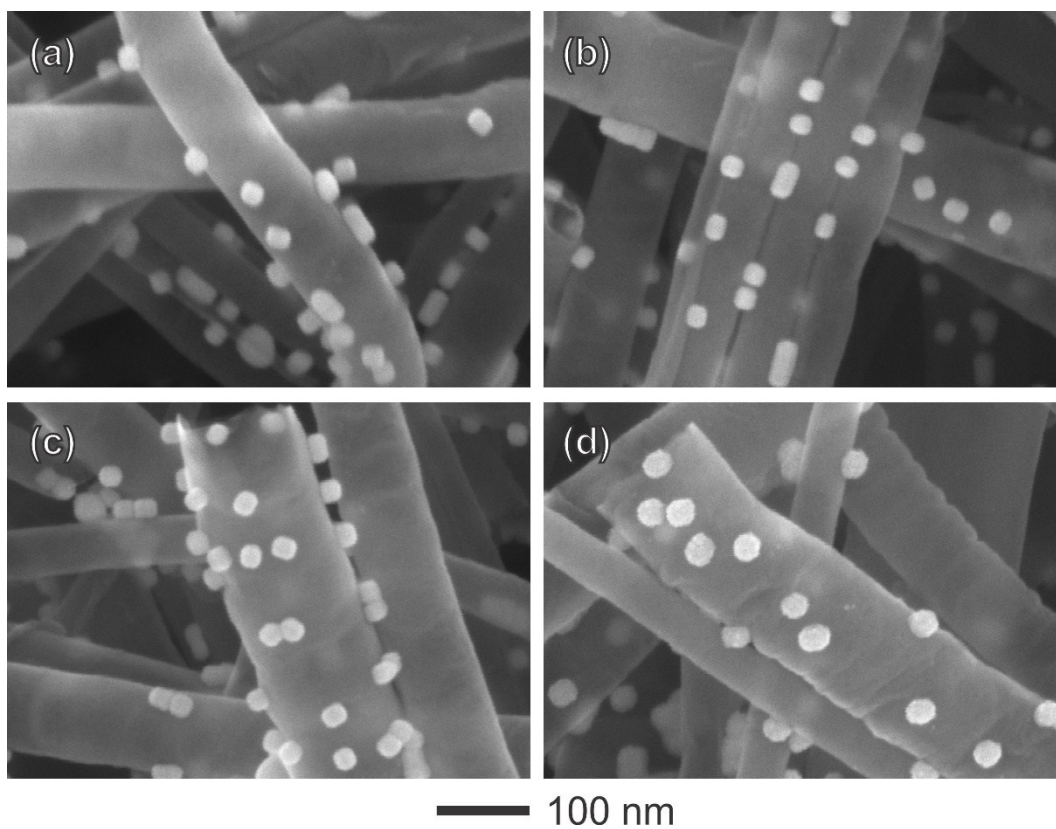


Fig. S6. SEM images of Pd@RuO_x nanocrystals on NCNT that were prepared by depositing Ru on Pd nanocubes/NCNT at various ALD cycles: (a) 10, (b) 20, (c) 30, and (d) 50 cycles, respectively.

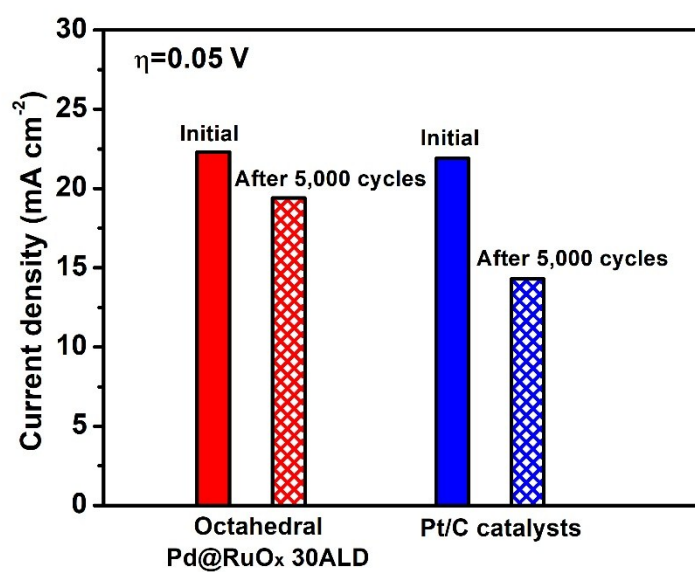


Fig. S7. Specific current activity at 0.05 V (versus RHE) of the octahedral Pd@RuO_x 30ALD and the Pt/C catalysts before and after 5,000 cycles durability test.

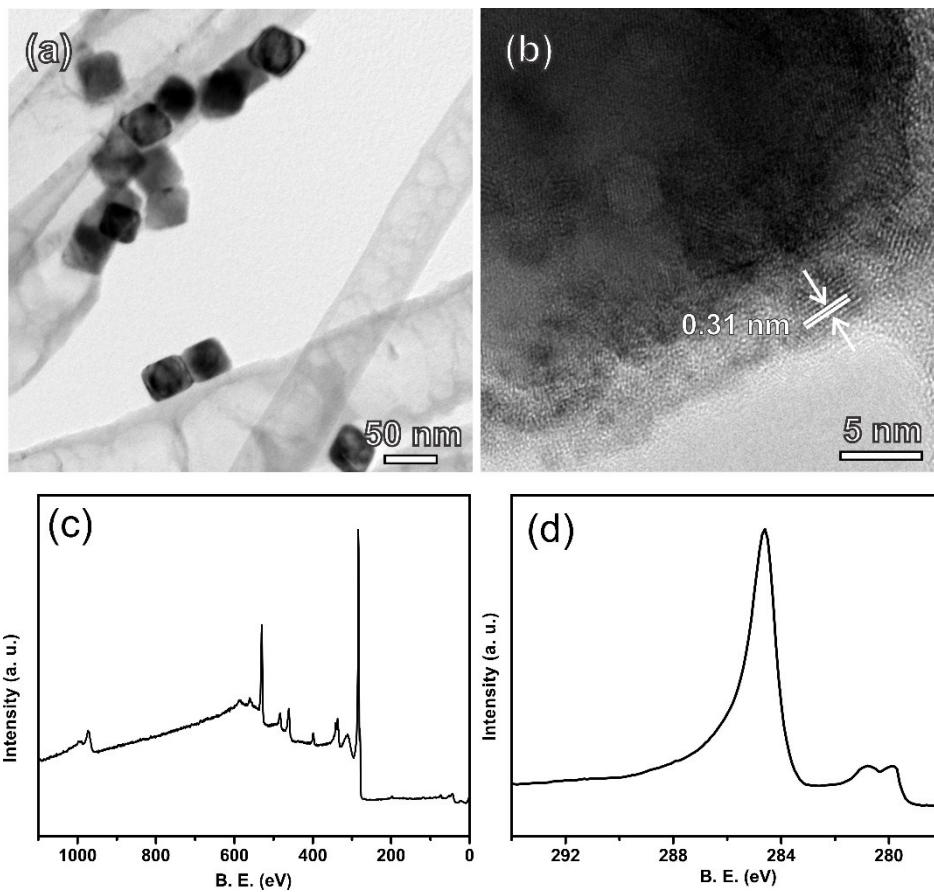


Fig. S8. TEM images and XPS spectra showing the structure of post-testing octahedral Pd@RuO_x 30ALD catalysts.

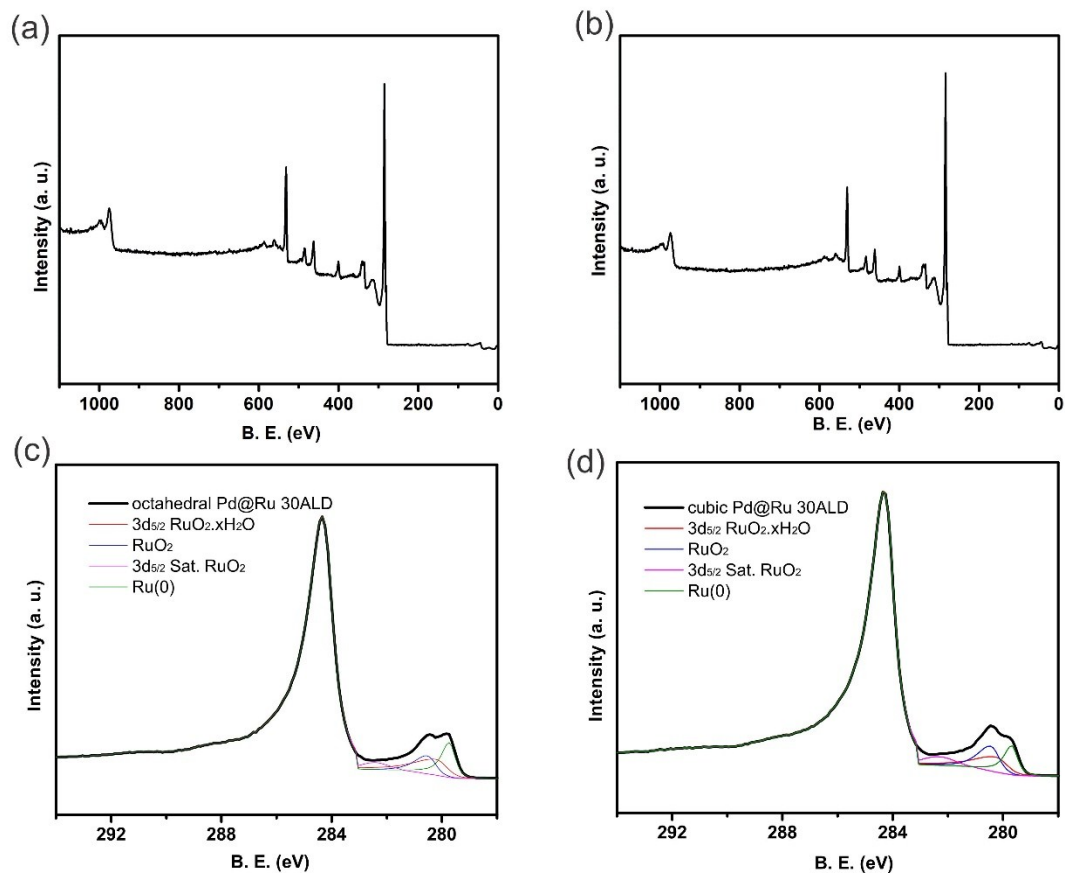


Fig. S9. XPS spectra showing the structure of Pd@RuO_x on NCNT catalysts.

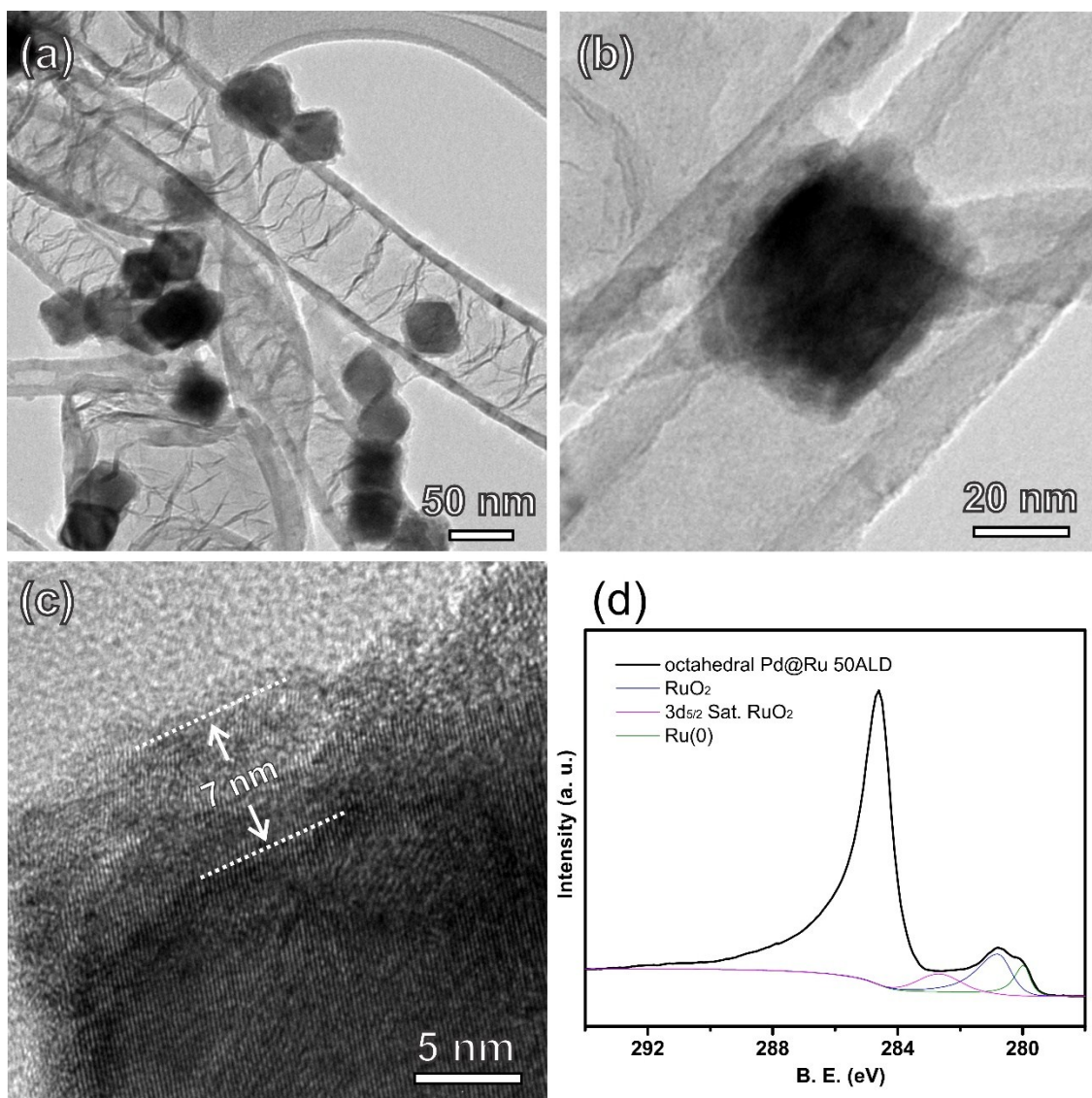


Fig. S10. TEM images and XPS spectra showing the structure of Pd@RuO_x 50ALD catalysts.

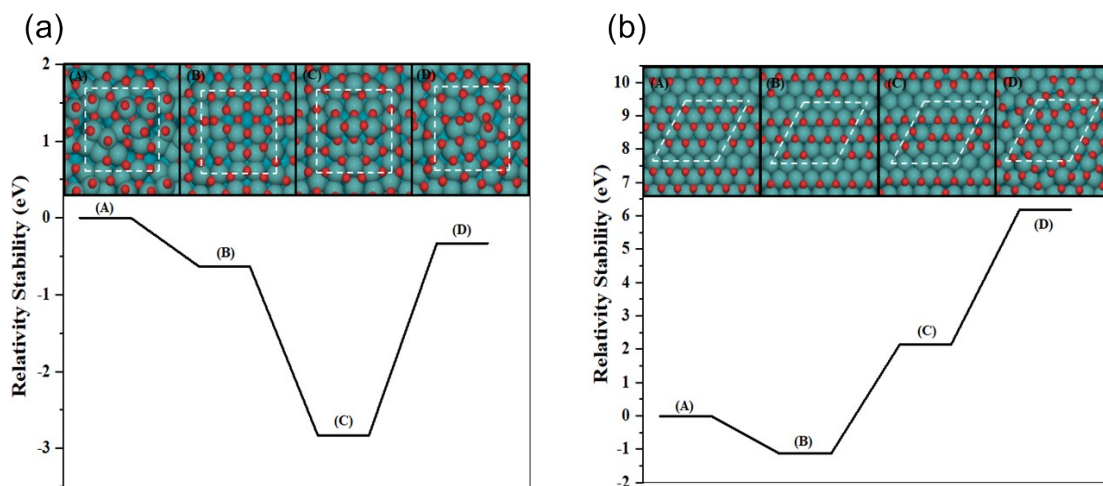


Fig. S11. Possible structures and relative stability for Pd@RuO_x (partially oxidized) (a) (100) surface and (b) (111) surface. (Ru atoms in blue, O atoms in red)

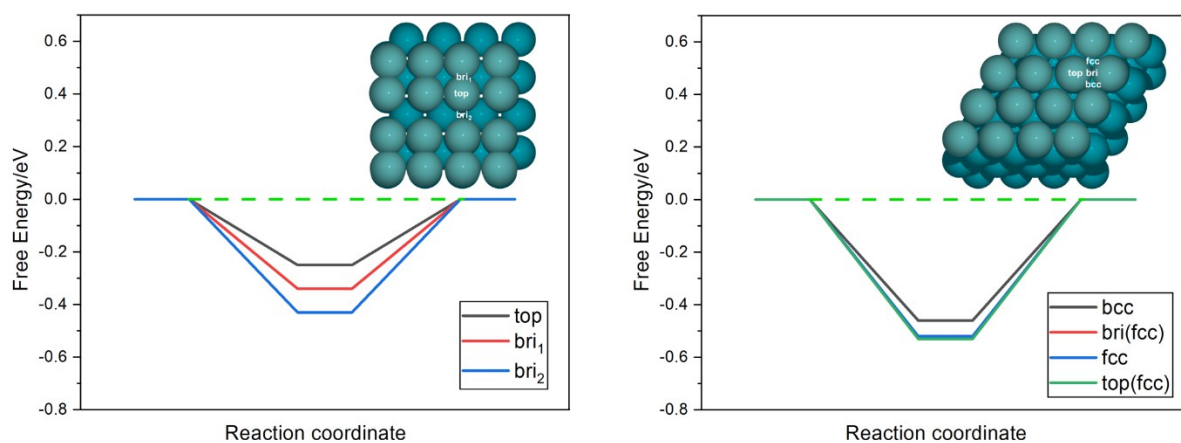


Figure S12. Free energy diagrams of possible reaction pathways for HER on metallic Ru phase on metal Pd (a) (100) surface and (b) (111) surface (“bri(fcc)” means the position where H is placed is bri, but the stable adsorption site is fcc site. “top(fcc) is the same)

Table S1. Comparison of HER performance of the as-prepared RuO_x on octahedral Pd/NCNT with state-of-art Ru-based catalysts.

| Catalyst | η (mV) @ 10 mA cm ⁻² | Electrolyte | Reference |
|--|---|--------------------------------------|---|
| Octahedral Pd@RuO _x 30ALD | 33 | 0.5 M H ₂ SO ₄ | Our work |
| Commercial Pt/C | 36 | 0.5 M H ₂ SO ₄ | Our work |
| Anomalous structured Ru on g-C ₃ N ₄ /C | ~680 | 0.5 M H ₂ SO ₄ | J. Am. Chem. Soc. 2016, 138, 16174–16181 |
| RuO ₂ nanowire on g-C ₃ N ₄ | 93 | 0.5 M H ₂ SO ₄ | ACS Appl. Mater. Interfaces 2016, 8, 28678–28688 |
| Anomalous structured Ru on g-C ₃ N ₄ /C | ~80 | 0.1 M KOH | J. Am. Chem. Soc. 2016, 138, 16174–16181 |
| RuO ₂ /Co ₃ O ₄ | 89 | 1 M KOH | RSC Adv. 2017, 7, 3686–3694 |
| Ru in mesoporous crystal TiO ₂ | 150 | 0.1 M KOH | J. Am. Chem. Soc. 2018, 140, 5719–5727 |

Table S2. Coordination number of Ru-Ru and Ru-O simulated from DFT.

| Catalysts | Model type | Coordination number (Ru-O) | Coordination number (Ru-Ru) | Bonding distance (A) (Ru-O) | Bonding distance (A) (Ru-Ru) | Ru(0) / % |
|---------------------|------------|----------------------------|-----------------------------|-----------------------------|------------------------------|-----------|
| Octahedral | 1 | 2.70 | 6.00 | 2.0122 | 2.7800 | 37.50 |
| Pd@RuO _x | 2 | 2.45 | 6.00 | 2.0030 | 2.8016 | 31.25 |
| with 30 Ru | 3 | 2.36 | 6.00 | 2.0227 | 2.8223 | 31.25 |
| ALD cycles | 4 | 2.60 | 6.00 | 2.0038 | 2.8134 | 37.50 |
| Cubic | 1 | 2.92 | 3.53 | 2.0339 | 2.7340 | 25.00 |
| Pd@RuO _x | 2 | 2.70 | 3.80 | 1.9522 | 2.7735 | 0 |
| with 30 Ru | 3 | 2.93 | 3.67 | 1.9787 | 2.8753 | 18.75 |
| ALD cycles | 4 | 2.93 | 4.40 | 1.9776 | 2.8812 | 12.50 |

Table S3. Active sites and Gibbs free-energy of hydrogen on (100) surface

| Active site | 1 | 2 | 3 | 4 | 5 | 6 | 7 |
|-----------------------|-------|-------|-------|-------|------|------|-------|
| ΔG_{H^*} (eV) | -0.13 | -0.15 | -0.65 | -0.34 | 0.04 | 0.38 | -0.50 |

Table S4. Active sites and Gibbs free-energy of hydrogen on (111) surface

| Active site | 1 | 2 | 3 | 4 | 5 | 6 | 7 | 8 | 9 | 10 |
|-----------------------|---|-------|-------|-------|------|-------|------|-------|-------|-------|
| ΔG_{H^*} (eV) | - | -0.07 | -0.06 | -0.06 | 0.09 | -0.06 | 0.07 | -0.06 | -0.04 | -0.04 |

0.16

Table S5. Active sites and Gibbs free-energy of hydrogen on pure Ru@Pd cubic

| Active site | top | bri ₁ | bri ₂ |
|-----------------------|-------|------------------|------------------|
| ΔG_{H^*} (eV) | -0.25 | -0.34 | -0.43 |

Table S6. Active sites and Gibbs free-energy of hydrogen on pure Ru@Pd octahedron

| Active site | bcc | bri(fcc) | fcc | top(fcc) |
|-----------------------|-------|----------|-------|----------|
| ΔG_{H^*} (eV) | -0.46 | -0.53 | -0.52 | -0.53 |